Closed-Form BER Results for MRC Diversity With Channel Estimation Errors in Ricean Fading Channels

Lingzhi Cao, *Member, IEEE*, and Norman C. Beaulieu, *Fellow, IEEE*

***Abstract*—Closed-form expressions for computing the average bit error rate (BER) for a class of modulation schemes in Ricean flat fading channels with maximal-ratio combining diversity and channel estimation errors are derived. The results are valid for a general multichannel model that includes Ricean and Rayleigh fading channels. The results are applicable to channel estimators that are jointly Gaussian with the channel gain. The BER performance of pilot symbol-assisted modulation is studied. The effects of estimation error on the diversity system are examined as well as the influences of varying the Ricean factor *K* and changing the number of diversity branches *L*.**

***Index Terms*—Diversity, estimation error, fading channels, maximal-ratio combining, pilot symbol-assisted modulation.**

I. Introduction

TWO-DIMENSIONAL (2-D) signaling constellations with perfect coherent detection have been well studied by many researchers [1]–[3]. Less work has considered the case where the coherent detection is subject to channel estimation errors. References [4]–[6] provided results for the symbol error rate (SER) when the estimation error is considered. The bit error rate (BER) for maximal-ratio combining (MRC) 16-quadrature amplitude modulation (16-QAM) with pilot symbol-assisted modulation (PSAM) estimation error in Rayleigh fading channels was derived in [4]. The results from [5] apply to both Rayleigh and Ricean fading channels but are limited to the case where the channel estimate is a minimum mean squared error (MMSE) estimate. Expressions for the SER of 2-D signaling in Rayleigh fading with MRC diversity and in Ricean fading without diversity were obtained in [6]. In this paper, we derive an exact BER expression for a class of 2-D signaling with MRC diversity in Ricean fading channels with estimation error. Our analysis can be applied to a general multichannel model [7].

II. System Model

Consider an MRC diversity system operating over L independent Ricean flat fading channels where the fading is assumed to be constant during a symbol duration T. The multichannel fading model follows the definition in [7]. The complex channel gain sample on the kth diversity branch can be expressed as

$$g_k = g_{\mathrm{I}k} + j g_{\mathrm{Q}k} = \alpha_k e^{j\theta_k} + \beta_k e^{j\phi_k} \tag{1}$$

where $g_{\mathrm{I}k}$ and $g_{\mathrm{Q}k}$ are the I and Q components of g_k, $\alpha_k e^{j\theta_k}$ is a line of sight (LOS) component with amplitude α_k and phase θ_k and can be considered as the mean m_{g_k} of g_k, and $\beta_k e^{j\phi_k}$ is the multipath scatter component where β_k is a Rayleigh-distributed amplitude with variance σ_g^2 and ϕ_k is uniformly distributed over $[0, 2\pi)$. Both Rayleigh and Ricean fading channels are included, and the LOS components of the branches can be different but the variances of the scatter components must be the same for different fading channels.

A received signal sample on the kth branch at the output of the matched filter is given by

$$r_k = g_k S_i + n_k \tag{2}$$

where S_i is the transmitted complex signal sample and n_k is an additive white Gaussian noise (AWGN) sample with variance σ_n^2 in both real and imaginary parts. We assume perfect synchronization and symbol timing recovery. The combiner output is a sum of L branch samples given by [8]

$$R = \sum_{k=1}^{L} \hat{g}_k^* r_k = \sum_{k=1}^{L} \hat{g}_k^* (g_k S_i + n_k) \tag{3}$$

where $\hat{g}_k$ is the complex channel estimate with mean $m_{\hat{g}}$ and second moment $\sigma_{\hat{g}}^2$. We assume that $\hat{g}_k$ and g_k are correlated complex Gaussian random variables. The combiner output phasor can also be presented in terms of the I component R_{I} and the Q component R_{Q} as

$$R = R_{\mathrm{I}} + j R_{\mathrm{Q}} \tag{4a}$$

$$R_{\mathrm{I}} = \frac{R + R^*}{2} \tag{4b}$$

$$R_{\mathrm{Q}} = -j \frac{R - R^*}{2}. \tag{4c}$$

Combining (4b) and (4c) with (3), we obtain

$$R_{\mathrm{I}} = \sum_{k=1}^{L} \left[\frac{1}{2} \hat{g}_k^* r_k + \frac{1}{2} (\hat{g}_k^* r_k)^* \right] \tag{5a}$$

$$R_{\mathrm{Q}} = \sum_{k=1}^{L} \left[\frac{-j}{2} \hat{g}_k^* r_k + \frac{-j^*}{2} (\hat{g}_k^* r_k)^* \right]. \tag{5b}$$

We consider 2-D modulation formats which have the property that the I and Q branches can be demodulated separately.

Manuscript received December 26, 2003; revised April 15, 2004; accepted April 30, 2004. The editor coordinating the review of this paper and approving it for publication is C. Xiao.

The authors are with the Department of Electrical and Computer Engineering, University of Alberta, Edmonton, AB T6G 2V4, Canada (e-mail: lingzhi@ee.ualberta.ca; beaulieu@ee.ualberta.ca).

Digital Object Identifier 10.1109/TWC.2005.850320

TABLE I
THE ERROR RATE FOR BINARY SIGNALS AFTER [9, eqs. (B-6), (B-7), AND (B-22)]

Fading	Diversity Order	$P_r(D<0)$
Rayleigh	1	$\frac{v_2}{v_1+v_2}$
Rayleigh	$L>1$	$\frac{1}{(1+v_2/v_1)^{2L-1}}\sum_{k=1}^{L}\binom{2L-1}{k}(\frac{v_2}{v_1})^k$
Ricean	1	$Q_1(a,b)-\frac{v_2/v_1}{1+v_2/v_1}I_0(ab)\exp[-\frac{1}{2}(a^2+b^2)]$
Ricean	$L>1$	$Q_1(a,b)-I_0(ab)\exp[-\frac{1}{2}(a^2+b^2)]+$ $\frac{I_0(ab)\exp[-\frac{1}{2}(a^2+b^2)]}{(1+v_2/v_1)^{2L-1}}\sum_{k=1}^{L}\binom{2L-1}{k}(\frac{v_2}{v_1})^k+$ $\frac{\exp[-\frac{1}{2}(a^2+b^2)]}{(1+v_2/v_1)^{2L-1}}\sum_{n=1}^{L-1}I_n(ab)\sum_{k=0}^{L-1-n}\binom{2L-1}{k}$ $\left[(\frac{b}{a})^n(\frac{v_2}{v_1})^k-(\frac{a}{b})^n(\frac{v_2}{v_1})^{2L-1-k}\right]$

Functions and Parameters	Definitions
$Q_m(a,b)$	the generalized Marcum's Q function
$I_n(x)$	the nth order modified Bessel function of the first kind
v_1	$\sqrt{w^2+\frac{1}{4(\mu_{xx}\mu_{yy}-\lvert\mu_{xy}\rvert^2)(\lvert C\rvert^2-AB)}}-w$
v_2	$\sqrt{w^2+\frac{1}{4(\mu_{xx}\mu_{yy}-\lvert\mu_{xy}\rvert^2)(\lvert C\rvert^2-AB)}}+w$
w	$\frac{A\mu_{xx}+B\mu_{yy}+C\mu_{xy}^*+C^*\mu_{xy}}{4(\mu_{xx}\mu_{yy}-\lvert\mu_{xy}\rvert^2)(\lvert C\rvert^2-AB)}$
a_{1k}	$2(\lvert C\rvert^2-AB)(\lvert\bar{X}_k\rvert^2\mu_{yy}+\lvert\bar{Y}_k\rvert^2\mu_{xx}-\bar{X}_k^*\bar{Y}_k\mu_{xy}-\bar{X}_k\bar{Y}_k^*\mu_{xy}^*)$
a_{2k}	$A\lvert\bar{X}_k\rvert^2+B\lvert\bar{Y}_k\rvert^2+C\bar{X}_k^*\bar{Y}_k+C^*\bar{X}_k\bar{Y}_k^*$
μ_{xy}	$\frac{1}{2}E[(X_k-\bar{X}_k)(Y_k-\bar{Y}_k)^*]$
a_1	$\sum_{k=1}^{L}a_{1k}$
a_2	$\sum_{k=1}^{L}a_{2k}$
a	$\left[\frac{2v_1^2v_2(a_1v_2-a_2)}{(v_1+v_2)^2}\right]^{1/2}$
b	$\left[\frac{2v_1v_2^2(a_1v_2+a_2)}{(v_1+v_2)^2}\right]^{1/2}$

Then every transmitted bit corresponds to W decision intervals on a one-dimensional (1-D) axis. The value of W depends on the transmitter modulation constellation. Every interval is delineated by two values d_{1w} and d_{2w} (1-D decision boundaries) with $w=1,\ldots,W$, where $d_{1w}<d_{2w}$, d_{1w} can be $-\infty$, and d_{2w} can be $+\infty$, corresponding to a particular symbol. In the receiver, after diversity combining, the decision boundaries are $\sum_{k=1}^{L}|\hat{g}_k|^2d_{1w}$ and $\sum_{k=1}^{L}|\hat{g}_k|^2d_{2w}$, respectively.

Our analysis will use a method for calculating the probability that a random variable D assumes values less than zero given in [9, Appendix B]. This method will be used in the sequel in the BER derivations. Denote

$$P_r=P(D<0)=\int_{-\infty}^{0}p(D)\mathrm{d}D \tag{6}$$

where $p(D)$ is the probability density function (pdf) of D. The pdf is derived by using the characteristic function of D. The variable D is a special case of the general quadratic form [9]

$$D=\sum_{k=1}^{L}\left(A|X_k|^2+B|Y_k|^2+CX_kY_k^*+C^*X_k^*Y_k\right) \tag{7}$$

where A, B, and C are complex constants, X_k and Y_k are correlated complex Gaussian random variables, and the L pairs $\{X_k,Y_k\}$ are independent. A closed-form expression for P_r is given in [9, eq. (B-21)], which requires the means $\bar{X}_k$ and $\bar{Y}_k$ and the second (central) moments μ_{xx}, μ_{xy} and μ_{yy} of X_k and Y_k. Note that the means of X_k and Y_k can be different for different channels, but the second (central) moments must be the same. Table I lists simplified expressions for P_r when X_k and Y_k both have zero means as well as the $L=1$ case.

Observe that (5) and the decision boundaries $\sum_{k=1}^{L}|\hat{g}_k|^2d_i$, where $d_i=d_{1w}$ or d_{2w}, can be expressed in the form of D in (7) by assigning $X_k=r_k$ and $Y_k=\hat{g}_k$, where $A=0$, $B=d_i$, and $C=1/2$ for the I component or $-(j/2)$ for the Q component. As we see, A and C are fixed; we only need to find the values of B that are decided by the decision boundaries for different constellations. As the constellations we consider are all symmetrical, we can examine only the I component R_{I}. Combined with (5a), the decision variable D can be written as

$$D=\sum_{k=1}^{L}B|\hat{g}_k|^2+R_{\mathrm{I}}=\sum_{k=1}^{L}\left(B|\hat{g}_k|^2+\frac{1}{2}r_k\hat{g}_k^*+\frac{1}{2}r_k^*\hat{g}_k\right). \tag{8}$$

The first- and second-order statistics of r_k and $\hat{g}_k$ can be obtained once an estimation technique is specified. The most common estimation methods that give an estimate having a joint Gaussian distribution with the estimated quantity are PSAM [4], [10], [11] and MMSE [5]. In this paper, we use the Doppler shift LOS model [12] to describe the Ricean fading channel and PSAM for estimation.

In a PSAM system, the channel estimate obtained from the pilot symbol in the mth frame $\hat{p}_m$ is given by [11]

$$\hat{p}_m = p_m + \frac{n_m}{s_p} \tag{9}$$

where p_m is the complex channel gain, n_m is an AWGN sample corrupting the received pilot symbol in the mth frame, and s_p is the known symbol inserted periodically into the first slot of a frame with length N. The fading at the nth symbol in the current frame on the kth diversity branch is estimated from M adjacent pilot symbols with M_1 pilot symbols from previous frames, one from the current frame, and M_2 pilot symbols from subsequent frames on the kth diversity branch, where $M_1 + M_2 + 1 = M$ [4]

$$\hat{g}_k^l = \sum_{m=-M_1}^{M_2} h_m^l \hat{p}_m = \sum_{m=-M_1}^{M_2} h_m^l \left(p_m + \frac{n_m}{s_p} \right) \tag{10}$$

and where h_m^l, $l = 0, 1, \ldots, N-1$, are the interpolation coefficients of the estimation filter [13]. The symbol location l has been omitted in the following equations for notational brevity.

In the Doppler shift LOS model [12]

$$\begin{aligned} m_{g_k} &= \alpha_k e^{j\theta_k} \\ &= \alpha_k \exp(2\pi f_m T l \cos\theta_{0k} + \phi_{0k}) \end{aligned} \tag{11a}$$

$$\begin{aligned} \Phi_{g_{\mathrm{I}k} g_{\mathrm{I}k}}(\Delta l) &= \sigma_g^2 J_0(2\pi f_m \Delta l T) \\ &\quad + \frac{\alpha_k^2}{2} \cos(2\pi f_m \Delta l T \cos\theta_{0k}) \end{aligned} \tag{11b}$$

$$\Phi_{g_{\mathrm{I}k} g_{\mathrm{Q}k}}(\Delta l) = \frac{\alpha_k^2}{2} \sin(2\pi f_m \Delta l T \cos\theta_{0k}) \tag{11c}$$

$$\Omega_k = \alpha_k^2 + 2\sigma_g^2 \tag{11d}$$

$$K_k = \frac{\alpha_k^2}{2\sigma_g^2} \tag{11e}$$

$$\bar{\gamma}_{bk} = \frac{\Omega_k E_b}{2\sigma_n^2} \tag{11f}$$

where $J_0(\cdot)$ is the zero-order Bessel function of the first kind [14], f_m is the maximum Doppler frequency, $f_m \cos\theta_{0k}$ is the Doppler shift, ϕ_{0k} is the random phase offset on the kth diversity branch, $\Delta l T$ is the time distance between the two symbols, Ω_k is the second moment of g_k, K_k is the Rice factor on the kth diversity branch, E_b is the average energy per bit, and $\bar{\gamma}_{bk}$ is the signal-to-noise ratio (SNR) per bit on the kth channel. Note that the amplitude of the mean of every diversity channel remains constant though the phase is rotating in the model.

In the case of PSAM, the means m_{r_k} and $m_{\hat{g}_k}$ and the second central moments $\mu_{r_k r_k}$, $\mu_{\hat{g}_k \hat{g}_k}$, and $\mu_{r_k \hat{g}_k}$ of r_k and $\hat{g}_k$ are given as

$$\begin{aligned} m_{r_k} &= m_{g_k} S_i \\ &= \alpha_k \exp(2\pi f_m T l \cos\theta_{0k} + \phi_{0k}) s_i \end{aligned} \tag{12a}$$

$$m_{\hat{g}_k} = \alpha_k \sum_{m=-M_1}^{M_2} h_m^l \exp(2\pi f_m T m N \cos\theta_{0k} + \phi_{0k}) \tag{12b}$$

$$\mu_{r_k r_k} = \sigma_g^2 |S_i|^2 + \sigma_n^2 \tag{12c}$$

$$\mu_{\hat{g}_k \hat{g}_k} = \sigma_g^2 \mathbf{H} \mathbf{X} \mathbf{H} + \frac{|H|^2 \sigma_n^2}{|s_p|^2} \tag{12d}$$

$$\mu_{r_k \hat{g}_k} = \sigma_g^2 S_i \sum_{m=-M_1}^{M_2} h_m^l J_0\left(2\pi f_m |mN - l| T \cos\theta_{0k}\right) \tag{12e}$$

$$\mathbf{H} = \left[h_{-M_1}^l, \ldots, h_{M_2}^l \right] \tag{12f}$$

$$X_{ij} = \sigma_g^2 J_0\left(2\pi f_m |i-j| N T_s\right) \tag{12g}$$

where $\mathbf{H}$ is the coefficient vector of the interpolation filter and X_{ij} is the ijth element of the covariance matrix $\mathbf{X}$. When there is no estimation error, the first and second central moments of $\hat{g}_k$ are given as

$$m_{\hat{g}_k} = m_{g_k} \tag{13a}$$

$$\mu_{\hat{g}_k \hat{g}_k} = \sigma_g^2 \tag{13b}$$

$$\mu_{r_k \hat{g}_k} = \sigma_g^2 s_i. \tag{13c}$$

In the following section, we derive BER expressions for binary phase-shift keying (BPSK), M-ary pulse-amplitude modulation (M-PAM), quaternary phase-shift keying (QPSK), and M-ary quadrature amplitude modulation (M-QAM).

III. Bit Error Probability

Refer to the detailed analysis in [9, Appendix B].

A. BPSK

Recall that BPSK is a 1-D modulation and the 1-D signal coordinate is either $s_0 = -\sqrt{E_b}$ or $s_1 = \sqrt{E_b}$. The decision threshold is zero. Thus, $B = 0$. Assuming that signal s_1 is transmitted, an error occurs when $R_{\mathrm{I}} < 0$. Recalling (5a), the BER for BPSK is then $P_{\mathrm{BPSK}} = P_{\mathrm{BPSK}|s_1} = P_r(R_{\mathrm{I}} < 0) = P_r(D_1 < 0)$ with $S_1 = s_1 = \sqrt{E_b}$ and $B = 0$.

B. PAM

Fig. 1 shows a 4-PAM constellation with Gray mapping in which $s_1 = -3d$, $s_2 = -d$, $s_3 = d$, and $s_4 = 3d$, where $d = (E_{s\mathrm{PAM}}/5)^{1/2}$ is the decision distance and $E_{s\mathrm{PAM}} = 2E_b$ is the average 4-PAM symbol energy. Every symbol is represented by two bits, one most significant bit (MSB) and one least significant bit (LSB). Assume that $s_3 = d$ or $s_4 = 3d$ has been sent. It is seen in Fig. 1 that the threshold for the

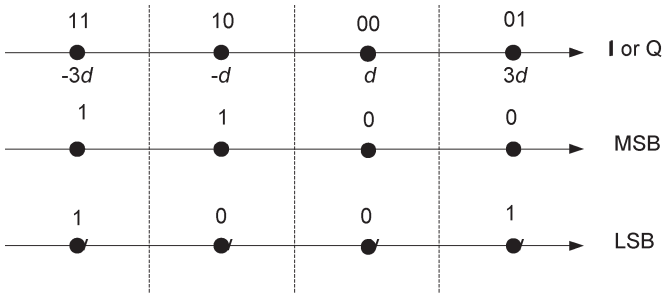

Fig. 1. 4-PAM/16-QAM I and Q bit demappings (after [11, Fig. 5]).

TABLE II
COEFFICIENTS IN THE BER EXPRESSION (16) FOR 4-PAM

i	w_i	x_i	z_i	i	w_i	x_i	z_i
1	1	3	0	4	-1	3	2
2	1	1	0	5	1	-1	2
3	1	3	-2	6	1	1	2

MSB is zero. Thus, $B = 0$. When s_3 has been sent, the BER of MSB is $P_r(D_1 < 0)$, where $S_1 = s_3 = d$ and $B = 0$ for decision variable D_1. When s_4 has been sent, the BER of MSB is $P_r(D_2 < 0)$, where $S_2 = s_4 = 3d$ and $B = 0$ for decision variable D_2. The average error rate for MSB is then

$$P_{\mathrm{MSB}} = \frac{1}{2}\left[P_r(D_1 < 0) + P_r(D_2 < 0)\right]. \tag{14}$$

For the LSB, it is seen in Fig. 1 that when $s_3 = d$ is sent, an error occurs when $R_{\mathrm{I}}|(s_3 = d) > \sum_{k=1}^{L} 2d|\hat{g}_k|^2$ or $R_{\mathrm{I}}|(s_3 = d) < -\sum_{k=1}^{L} 2d|\hat{g}_k|^2$. Due to the symmetry of the constellation, the probability $P_r(R_{\mathrm{I}} > \sum_{k=1}^{L} 2d|\hat{g}_k|^2)$ when $s_3 = d$ is transmitted is equal to $P_r(R_{\mathrm{I}} < -\sum_{k=1}^{L} 2d|\hat{g}_k|^2)$ when $s_2 = -d$ is transmitted, again seen in Fig. 1. The probability that an error occurs is obtained as $P_r(R_{\mathrm{I}}|(s_2 = -d) < -\sum_{k=1}^{L} 2d|\hat{g}_k|^2) + P_r(R_{\mathrm{I}}|(s_3 = d) < -\sum_{k=1}^{L} 2d|\hat{g}_k|^2)$. We set $D_3 = R_{\mathrm{I}}|(s_2 = -d) + \sum_{k=1}^{L} 2d|\hat{g}_k|^2$ where $S_3 = s_2 = -d$ and $B = 2d$, and $D_4 = R_{\mathrm{I}}|(s_3 = d) + \sum_{k=1}^{L} 2d|\hat{g}_k|^2$ where $S_4 = s_3 = d$ and $B = 2d$. When $s_4 = 3d$ is transmitted, an error occurs when $-\sum_{k=1}^{L} 2d|\hat{g}_k|^2 < R_{\mathrm{I}} < \sum_{k=1}^{L} 2d|\hat{g}_k|^2$. The probability of error is then $P_r(R_{\mathrm{I}}|(s_4 = 3d) < \sum_{k=1}^{L} 2d|\hat{g}_k|^2) - P_r(R_{\mathrm{I}}|(s_i = 3d) < -\sum_{k=1}^{L} 2d|\hat{g}_k|^2)$. We set $D_5 = R_{\mathrm{I}}|(s_4 = 3d) - \sum_{k=1}^{L} 2d|\hat{g}_k|^2$ where $S_5 = s_4 = 3d$ and $B = -2d$, and $D_6 = R_{\mathrm{I}}|(s_4 = 3d) + \sum_{k=1}^{L} 2d|\hat{g}_k|^2$ where $S_6 = s_4 = 3d$ and $B = 2d$.

Thus, the average BER for the LSB is

$$P_{\mathrm{LSB}} = \frac{1}{2}\left\{\left[P_r(D_3 < 0) + P_r(D_4 < 0)\right] + \left[P_r(D_5 < 0) - P_r(D_6 < 0)\right]\right\}. \tag{15}$$

Combining (14) and (15), the BER for 4-PAM can be expressed as

$$P_{4-\mathrm{PAM}} = \frac{1}{2}(P_{\mathrm{MSB}} + P_{\mathrm{LSB}}) = \frac{1}{4}\sum_{i=1}^{6} w_i P_r(D_i < 0) \tag{16}$$

TABLE III
COEFFICIENTS IN THE BER EXPRESSION (17) FOR 16-QAM

i	w_i	x_i	y_i	z_i	i	w_i	x_i	y_i	z_i
1	1	3	3	0	7	-1	3	3	2
2	1	3	1	0	8	-1	3	1	2
3	1	1	3	0	9	1	-1	3	2
4	1	1	1	0	10	1	-1	1	2
5	1	3	3	-2	11	1	1	3	2
6	1	3	1	-2	12	1	1	1	2

where $S_i = x_i d$ in (2), $B_i = z_i d$ in decision variable D_i, and w_i, x_i, and z_i are listed in Table II.

C. QPSK

A QPSK symbol can represent four signal constellation points with 2 bits, "01," "11," "10," and "00," corresponding to four different phases, for example, $\pi/4$, $3\pi/4$, $5\pi/4$, and $7\pi/4$. The complex representation of a QPSK signal point is $s_t = (E_{s\mathrm{QPSK}})^{1/2}\exp\{j[(2t-1)/4]\pi\}$, where $t = 1, 2, 3, 4$ and $E_{s\mathrm{QPSK}} = 2E_b$ is the average QPSK symbol energy. It can be implemented by transmitting two BPSK signals at the same time on the I and Q branches. Thus, the demodulation and decision on each branch are the same as for the BPSK described in Section III-A. The BER for QPSK is then very similar to that for BPSK and is given by $P_{\mathrm{QPSK}} = P_r(D_1 < 0)$ with $S_1 = s_1 = (E_{s\mathrm{QPSK}})^{1/2}\exp[j(1/4)\pi]$ and $B = 0$. Note that the cross-quadrature intersymbol interference caused by imperfect estimation has been accounted for in (5a), (5b), and (8).

D. M-QAM

An M-QAM signal is obtained by transmitting M-PAM signals on the I and Q channels. Here, we use 16-QAM as an example. The complex signal point can be represented as $s_t = x_t d + j y_t d$, where x_t, $y_t = \pm 1$ or ± 3 and $t = 1, 2, \ldots, 16$, $d = (E_{s\mathrm{QAM}}/10)^{1/2}$ is the decision distance, and $E_{s\mathrm{QAM}} = 4E_b$ is the average 16-QAM symbol energy. We consider only the symbols in the first quadrant due to constellation symmetry [15, Fig. 3.3]. Note that this method is only applied to constellations with Gray mapping. The decision criterion on each quadrature channel is the same as that of 4-PAM, described in Section III-B, but we need to consider the cross-quadrature interference component due to the imperfect estimation. When the value of x_t is fixed, there are two choices for the value of y_t, 1 or 3. Thus, the BER for 16-QAM can be obtained as

$$P_{16-\mathrm{QAM}} = \frac{1}{8}\sum_{i=1}^{12} w_i P_r(D_i < 0) \tag{17}$$

where $S_i = x_i d + j y_i d$ in (2), $B_i = z_i d$ in decision variable D_i, and w_i, x_i, y_i, and z_i are listed in Table III.

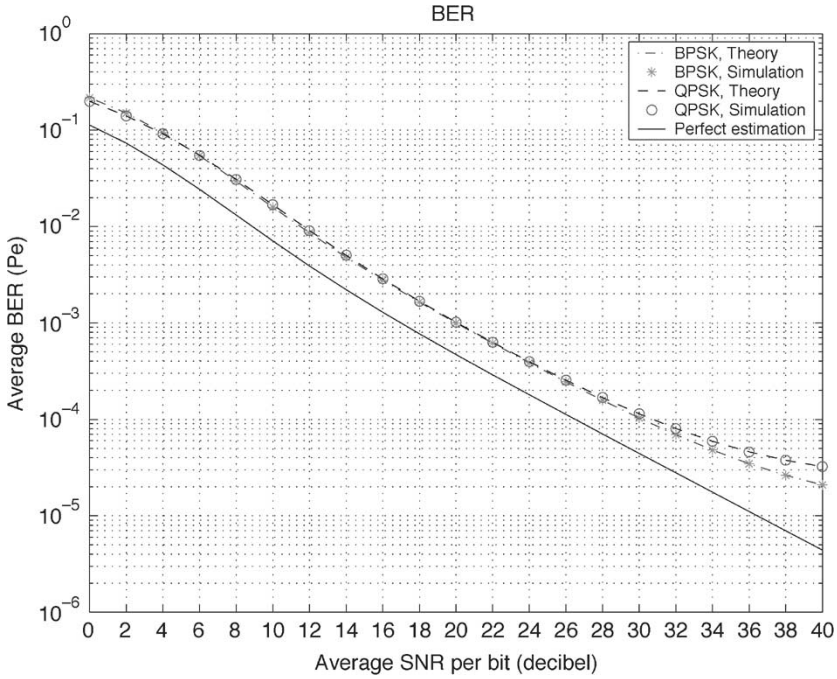

Fig. 2. BER of BPSK and QPSK with $L = 1$ and $K = 5$ dB.

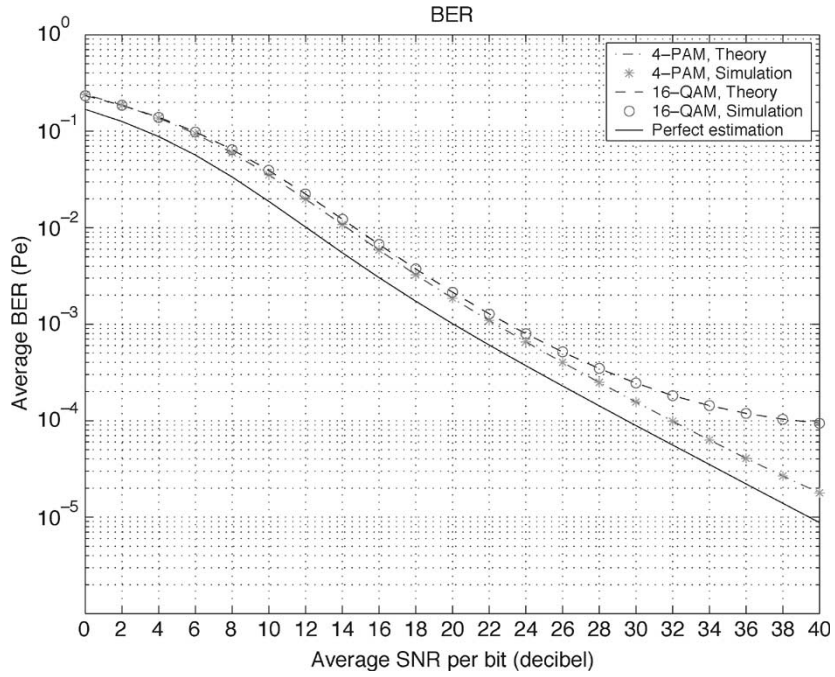

Fig. 3. BER of 4-PAM and 16-QAM with $L = 1$ and $K = 5$ dB.

Some examples are given in the next section; the computed BERs include the influences of estimation error, MRC diversity, and the LOS component on the system performances.

IV. Examples

All the theoretical results and simulations are implemented in Matlab. For convenience of computation and discussion, we set $K_k = K$, $\theta_{0k} = 0$, and $\phi_{0k} = 0$ for all the diversity branches. Thus, the average SNR $\bar{\gamma}_{bk}$ is the same on all the diversity channels. Note importantly that our results are applied to the multichannel with different specular components but with the same scattering variance. The system parameters are set as follows: frame length $N = 15$, interpolation order $M = 30$ with $M_1 = 14$ and $M_2 = 15$, symbol location $l = 8$, maximal normalized Doppler shift $f_m T = 0.03$, and the fading variance $\sigma_g^2 = 1$. The sinc interpolator is implemented with a Hamming window [13].

Figs. 2 and 3 show the BERs of BPSK, QPSK, 4-PAM, and 16-QAM for single-branch reception over a Ricean flat

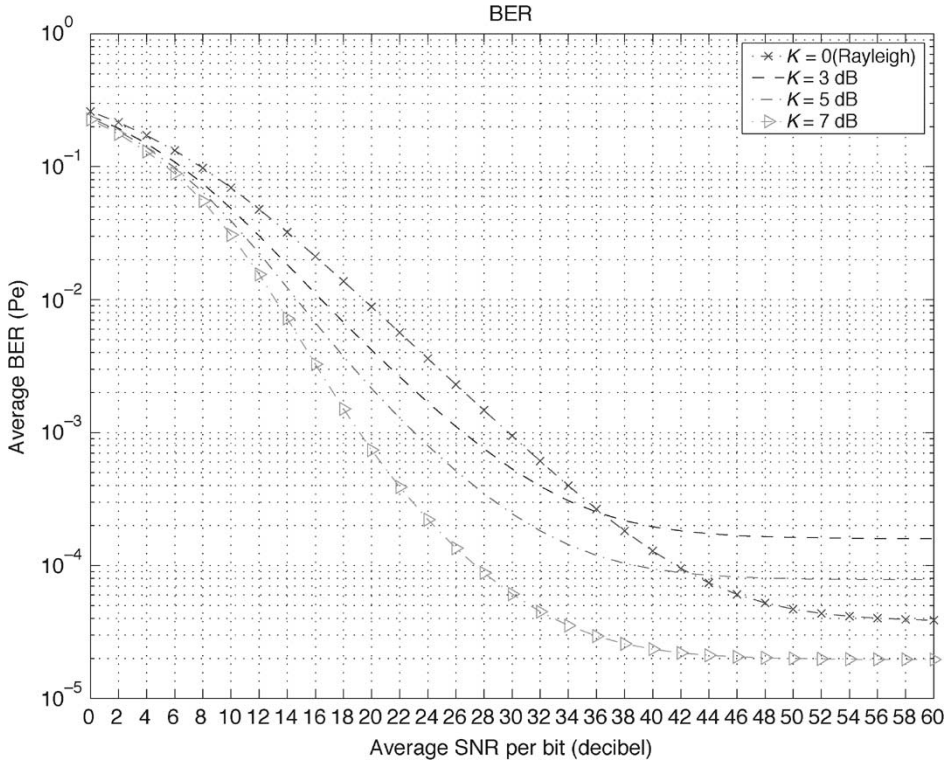

Fig. 4. BER of single-branch reception 16-QAM for different values of K.

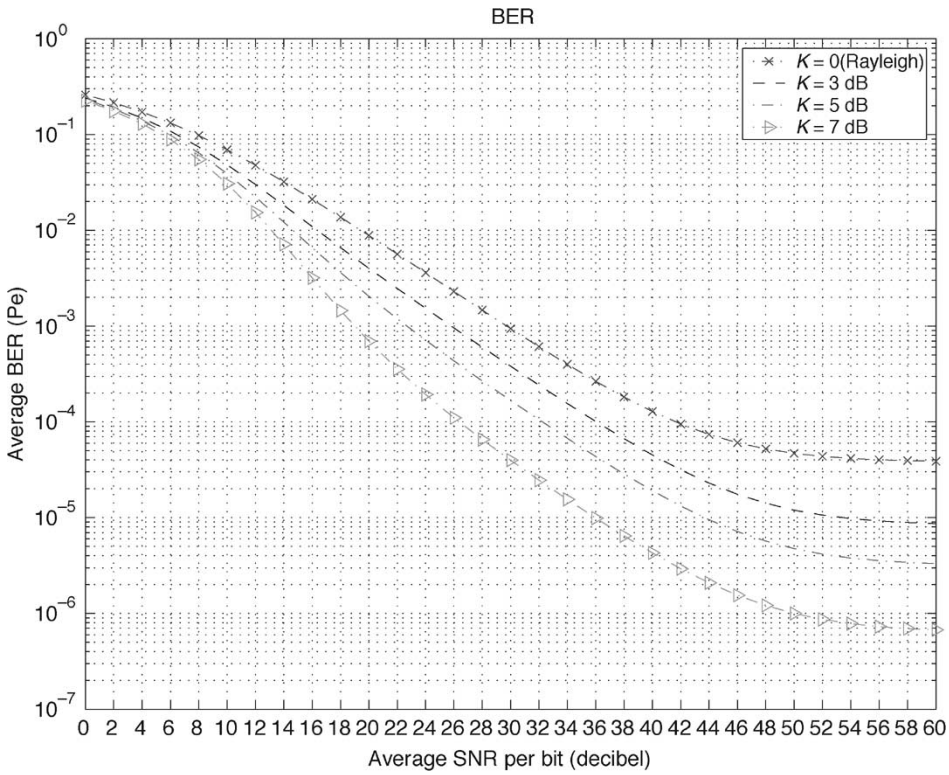

Fig. 5. BER of single-branch reception 16-QAM for different values of K when the means of all diversity branches are constant.

fading channel with Rice factor $K = 5$ dB. Both theoretical and simulation results are presented and are in excellent agreement. The BER performances are the same for BPSK and QPSK, as they are also for 4-PAM and 16-QAM, respectively, when the channel is perfectly known. However, it is seen in Figs. 2 and 3 that when there is an estimation error, the BERs of QPSK and 16-QAM are worse than those of BPSK and 4-PAM, particularly as $\bar{\gamma}_b$ increases due to the cross-quadrature interference caused by the imperfect channel estimation.

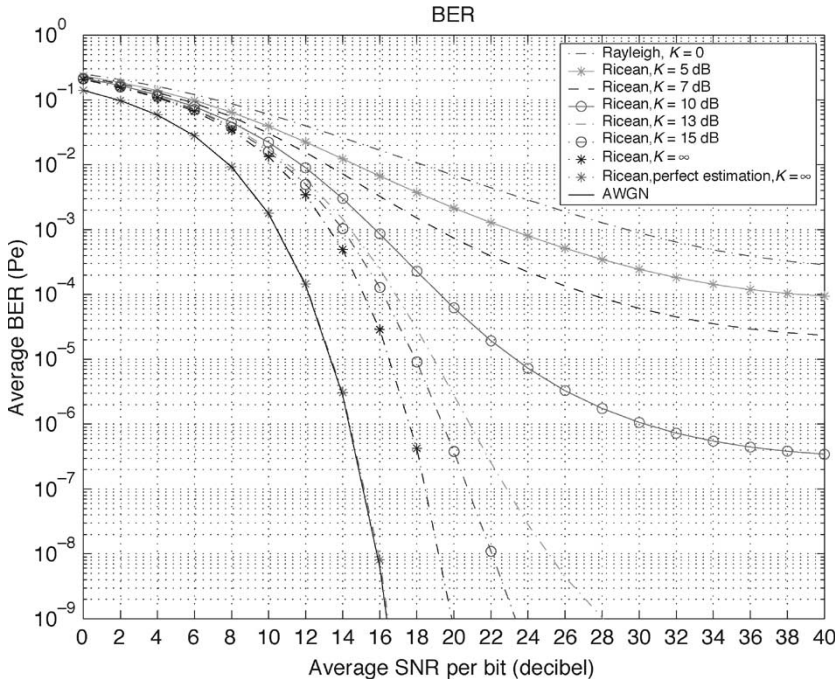

Fig. 6. BER of single-branch reception 16-QAM for different values of K.

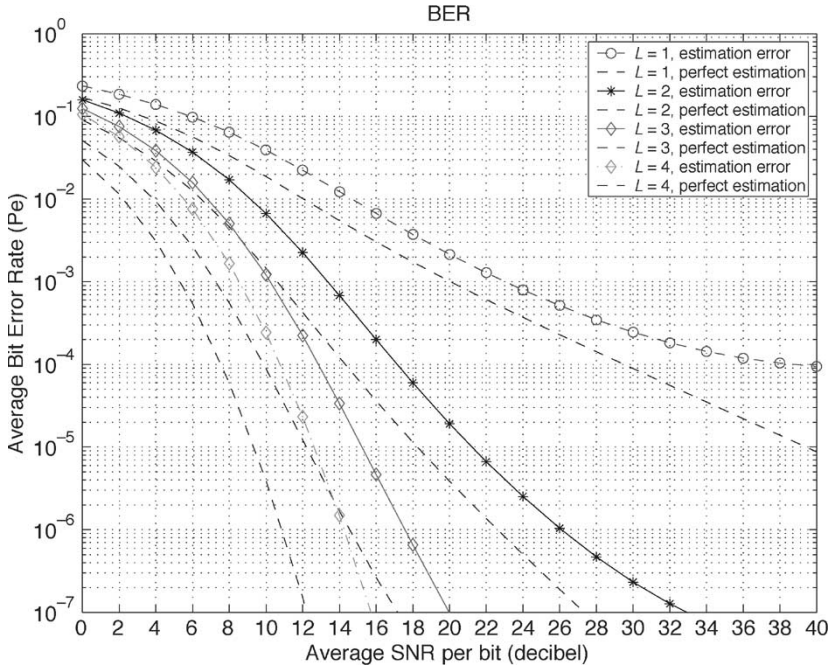

Fig. 7. BER of diversity 16-QAM with $K = 5$ dB.

We use 16-QAM as an example. Fig. 4 shows the BERs of single-branch reception 16-QAM for different values of K with imperfect channel estimation for the range of SNR values (0–60 dB).We compare the BER in Rayleigh fading $(K = 0)$ with that in Ricean fading. When the values of K are less than about 7 dB, the BER in Ricean fading is better (smaller) for small to large values of SNR but becomes worse (larger) than that in Rayleigh fading for very large SNR when the error floor occurs. This result may seem surprising and contrary to previous results. It is not; rather, it is a consequence of the Ricean fading model that we have employed that has a mean with constant amplitude but a rotating phase. Most past work assumes a simpler Ricean fading model that has constant (amplitude and phase) mean. In Fig. 5, we show the BER performance where we use the simple Ricean model [12]. In this model, the mean of the channel gain is fixed instead of having a constant amplitude and rotating phase as was the case in Fig. 4. In this case, the performance when an LOS component

exists is always better than the Rayleigh case. It appears that the errors introduced by estimating a changing mean (rather than a constant mean) cause the system performance with a weak LOS component to become worse than that in Rayleigh fading channels.

Fig. 6 shows the BERs of 16-QAM for different values of K. The BER in an AWGN channel ($K = \infty$) is also presented for comparison. When there is no channel estimation error, the BER in an AWGN channel is the same as that in Ricean fading with a very large K, as expected. However, there is always a gap between the BER in the Ricean fading channel and that in the AWGN channel when estimation error exists, no matter how large K is.

Fig. 7 presents the BER performance of MRC 16-QAM with $K = 5$ dB. Both BERs for perfect channel estimation and imperfect channel estimation are shown for comparison. As expected, the diversity gain increases in both perfect and imperfect cases with increasing numbers of diversity branches and shows diminishing returns as the diversity order increases. However, we can see in Fig. 7 that the differences between the BERs with perfect channel estimation and imperfect channel estimation increase with increasing numbers of diversity branches.

V. Conclusion

Closed-form expressions for the BERs of MRC BPSK, QPSK, 4-PAM, and 16-QAM with PSAM channel estimation in Ricean flat fading channels have been derived. The results can be extended to other estimation methods when the channel estimate is jointly Gaussian with the channel gain. They can also be applied to general M-QAM. The system performance has been analyzed for different values of Ricean factor K and numbers of diversity branches. The effects of channel estimation error have also been studied.

References

[1] M. K. Simon and M.-S. Alouini, "A unified approach to the performance analysis of digital communication over generalized fading channels," *Proc. IEEE*, vol. 86, no. 9, pp. 1860–1877, Sep. 1998.

[2] X. Dong, N. C. Beaulieu, and P. H. Wittke, "Signaling constellations for fading channels," *IEEE Trans. Commun.*, vol. 47, no. 5, pp. 703–714, May 1999.

[3] S. Chennakeshu and J. B. Anderson, "Error rates for Rayleigh fading multichannel reception of MPSK signals," *IEEE Trans. Commun.*, vol. 43, no. 2/3/4, pp. 338–346, Feb./Mar./Apr. 1995.

[4] L. Cao and N. C. Beaulieu, "Exact error rate analysis of diversity 16-QAM with channel estimation error," *IEEE Trans. Commun.*, vol. 52, no. 6, pp. 1019–1029, Jun. 2004.

[5] M. G. Shayesteh and A. Aghamohammadi, "On the error probability of linearly modulated signals on frequency-flat Ricean, Rayleigh, and AWGN channels," *IEEE Trans. Commun.*, vol. 43, no. 2/3/4, pp. 1454–1466, Feb./Mar./Apr. 1995.

[6] S. K. Wilson and J. M. Cioffi, "Probability density functions for analyzing multi-amplitude constellations in Rayleigh and Ricean channels," *IEEE Trans. Commun.*, vol. 47, no. 3, pp. 380–386, Mar. 1999.

[7] W. C. Lindsey, "Error probabilities for Rician fading multichannel reception of binary and n-ary signals," *IEEE Trans. Inf. Theory*, vol. 10, no. 4, pp. 339–350, Oct. 1964.

[8] M. J. Gans, "The effect of Gaussian error in maximal ratio combiners," *IEEE Trans. Commun. Technol.*, vol. 19, no. 4, pp. 492–500, Aug. 1971.

[9] J. G. Proakis, *Digital Communications*, 4th ed. New York: McGraw-Hill, 2001.

[10] J. K. Cavers, "An analysis of pilot symbol assisted modulation for Rayleigh fading channels," *IEEE Trans. Veh. Technol.*, vol. 40, no. 4, pp. 1389–1399, Nov. 1991.

[11] X. Tang, M.-S. Alouini, and A. J. Goldsmith, "Effect of channel estimation error on M-QAM BER performance in Rayleigh fading," *IEEE Trans. Commun.*, vol. 47, no. 12, pp. 1856–1864, Dec. 1999.

[12] G. L. Stuber, *Principles of Mobile Communication*, 2nd ed. Norwell, MA: Kluwer, 2001.

[13] Y.-S. Kim, C.-J. Kim, G.-Y. Jeong, Y.-J. Bang, H.-K. Park, and S. S. Choi, "New Rayleigh fading channel estimator based on PSAM channel sounding technique," in *Proc. IEEE Int. Conf. Communications (ICC)*, Montreal, QC, Canada, Jun. 1997, pp. 1518–1520.

[14] *Handbook of Mathematical Functions with Formulas, Graphs, and Mathematical Tables*, M. Abramowitz and I.A. Stegun, Eds. New York: Dover, 1974.

[15] L. Hanzo, T. Webb, and T. Keller, *Single- and Multi-Carrier Quadrature Amplitude Modulation: Principles and Applications for Personal Communications, WLANs and Broadcasting*. Chinchester, U.K.: Wiley, 2002.